Int. J Heat Mass Transfer. Vol. 30, No 2, pp. 379–393, 1987
Printed in Great Britain

0017–9310/87 $3.00 + 0.00
Pergamon Journals Ltd.

Leidenfrost boiling of methanol droplets on hot porous/ceramic surfaces

C. T. AVEDISIAN and J. KOPLIK*

Sibley School of Mechanical and Aerospace Engineering, Cornell University, Ithaca, NY 14853, U.S.A.

(*Received* 8 *August* 1985 *and in final form* 5 *June* 1986)

Abstract—An experimental and analytical study of film boiling methanol droplets on a porous/ceramic surface is reported. Droplet evaporation times in the wetting and film boiling regimes were measured on a polished stainless-steel surface and three ceramic/alumina surfaces of 10%, 25%, and 40% porosity. It was found that the Leidenfrost temperatures increased as surface porosity increased. The Leidenfrost point of the 10% and 25% porous surfaces were nearly 100 K higher and 200 K higher, respectively, than that of the polished stainless-steel surface; methanol droplets could not be levitated on the 40% porous surface at surface temperatures as high as 620 K, which was the maximum surface temperature which could be imposed on this particular material with our apparatus. The evaporation time of liquid deposited on this surface was thus almost two orders of magnitude lower than for levitated droplets on the three other surfaces tested at the same temperature. In the Leidenfrost regime droplets evaporated faster on the porous surfaces than on the stainless-steel surface, and the evaporation time decreased with increasing surface porosity at the same surface temperature. The reduced evaporation times were thought to have their origin in a decrease of the vapor film thickness separating the droplet from the ceramic surface due to vapor absorption and flow within the ceramic material. An analysis of flow in a horizontal channel bounded by an impermeable wall above and a permeable wall of finite thickness below was used to model the film boiling process. The results provided a basis for correlating our evaporation time measurements.

1. INTRODUCTION

FILM boiling of liquid droplets at hot surfaces is of current technological importance for its relevance to droplet combustion, spray cooling of hot surfaces, and ln g spills on water. Previous work has employed a variety of pure liquids, mixtures, emulsions, and solid suspensions [1–9]. The surfaces used in these studies were impermeable. Recent interest in ceramic engines, and more fundamental problems involving liquids in contact with porous materials, creates the possibility that surfaces with which droplets in a spray might interact would be porous. In this event, some of the vapor evaporated from the side of the droplet adjacent to the surface would be absorbed or percolated in the porous matrix. The thickness of the vapor film separating the droplet from the surface then decreases compared to evaporation above an impermeable surface, with a consequent increase in the heat transfer rate to the droplet and decrease in the droplet evaporation time. Also, certain ceramic materials can catalyze exothermic reactions. The chemical heat release could then also increase the total heat transfer rate to the droplet, and again reduce its evaporation time.

The purpose of the present work was to (1) measure the evaporation times and Leidenfrost temperatures of liquid droplets in film boiling on horizontal porous surfaces; and (2) develop a simple model which could be used as a basis for correlating our observations. Four surfaces were studied: polished stainless-steel, and three ceramic/alumina (Al_2O_3) surfaces of 10%, 25%, 40% porosity (hereinafter referred to as the P1, P2 and P3 surfaces, respectively). Methanol was selected as the test liquid because of the possibility of catalyzing an exothermic reaction of methanol vapor at an alumina surface—conversion of methanol to dimethylether [10]—though results did indicate that such a catalytic effect was probably not operative during our experiment. To isolate the effects of surface porosity, the initial droplet subcooling (about 5 K), ambient pressure (0.101 MPa), and initial droplet volume (11.8 μl) were held constant. The primary variable was the temperature of the porous surface.

2. EXPERIMENT

2.1. *Apparatus and procedure*

A schematic diagram of the apparatus is shown in Fig. 1. Primary components were: (1) the heater block (cylindrical copper billet 6.4 cm diameter and 10.8 cm long containing five symmetrically located cylindrical cartridge heaters—Hotwatt cat. no. S254); (2) removable test surface 1.5 cm thick attached to the end of the copper billet; (3) droplet injector; and (4) video optical system.

The heaters were wired through a parallel circuit whose potential and current were controlled through an analog temperature controller. Droplets (11.8 ± 0.1 μl volume) were deposited on the test surfaces by a syringe fitted with a flat-tipped 18 gage needle. The needle tip was positioned 5 mm above the center of the surface in all experiments, and the plunger progressively depressed until a droplet detached by its own weight.

Surface temperatures of the polished stainless-steel disk were determined by extrapolating the tempera-

* Present address: Division of Engineering, Brown University, Providence, RI 02912, U.S.A.

NOMENCLATURE

a_i	constant in velocity field in vapor film ($i = 1, 2$), equation (8)
b_i	constant in porous medium velocity field ($i = 1, 2$), equation (8)
B	defined by equation (14)
C	empirical constant, equation (18)
C_0	proportionality constant for permeability, equation (16)
C_{ps}	solid thermal conductivity
f_1	volume truncation factor for an oblate spheroid
f_2	surface area truncation factor for an oblate spheroid
g	gravitational constant
h	thickness of the porous surface
h_{fg}	latent heat of vaporization
k_g	vapor thermal conductivity
k_s	solid thermal conductivity
$\bar{k}$	permeability
k	$\equiv \bar{k}/\phi$
l	characteristic particle dimension for permeability in equation (16)
P	pressure in the vapor film
P_0	ambient pressure surrounding the droplet
R_0	base radius of droplet (Fig. 6)
t_e	total droplet evaporation time
T_s	temperature of the hot surface
T_{s0}	initial surface temperature, $\equiv T_s(t = 0)$
T_b	droplet temperature (338 K at 0.101 MPa)
T_{Leid}	Leidenfrost temperature
u	vapor velocity in the porous surface
v	gas velocity in the vapor film
V	liquid volume
V_0	initial liquid volume
x	radial position from droplet center
y	distance normal to the hot surface.

Greek symbols

α	thermal diffusivity
γ	emissivity
δ	thickness of the vapor film
ΔT	$\equiv T_s - T_b$
ε	ratio of velocity gradients at interface of porous surface and vapor film, equation (5c)
ζ	$\equiv h/k^{1/2}$
μ_g	vapor viscosity
ξ	defined by equation (19)
ρ_g	vapor density
ρ_l	liquid density
σ	Stefan–Boltzmann constant
ϕ	surface porosity.

ture recorded at three locations within the disk. Extrapolated surface temperatures were found to be within 0.5 K of the temperature recorded by the uppermost thermocouple (located 0.8 mm below the center). The thermocouples were made from 36 gage, glass-braid-sheated chromel–alumel wire. Surface temperatures of the ceramic surfaces were measured via a fine gage (0.03 mm bead) thermocouple bonded near the centroid of the surface by ceramic cement.

A clear video record of the evaporation process was obtained by videotape with an RCA black and white video camera (model T2010) fitted with a Nikon 55 mm macro lens. Light was supplied from a single GE FHX bulb fitted with heat absorbing glass. An electronic timer with a resolution of 0.1 s added a stop clock image to the video display.

At each surface temperature selected, several droplets were sequentially deposited and their evaporation times recorded. Sufficient time was allotted between successive drops for the test surface to regain thermal

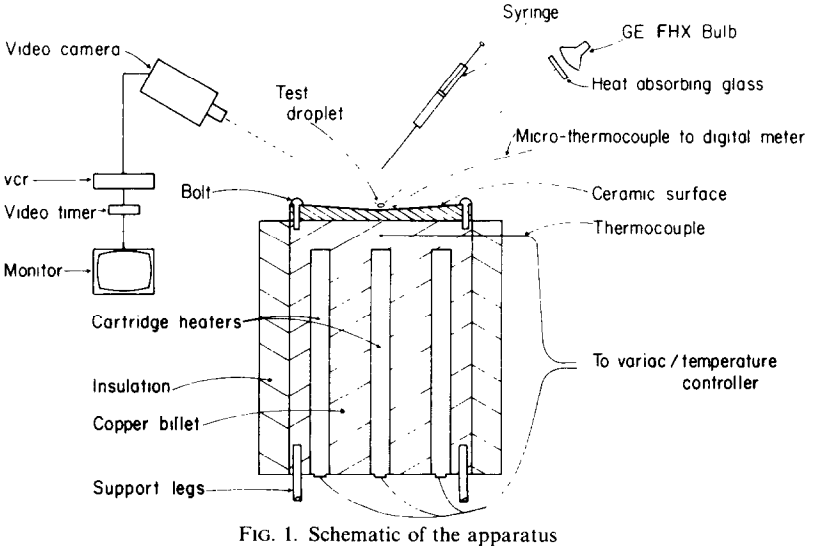

FIG. 1. Schematic of the apparatus

equilibrium. Continuous and precise control of the surface temperature was limited by the resolution of the controller. Temperature increments of 15–25 K were chosen and evaporation times recorded at each temperature. When variations of the evaporation time with surface plate temperature were very small, larger temperature increments were taken. This was done to avoid taking uninformative measurements, and occurred mostly with the P3 surface (between 515 and 616 K).

2.2. *Surfaces studied*

(a) *Stainless-steel.* The stainless-steel surface was a circular disk 1.7 cm thick and 6.4 cm diameter with mounting holes drilled around its periphery. A 1° conical depression was machined in the central 4 cm of the surface to prevent a droplet from sliding off. The surface was initially polished to a mirror finish.

Figure 2a illustrates a 35 mm photograph and electron micrograph (1000×) of this surface. The linear edges visible in Fig. 2a are machining marks.

(b) 10% *porous/alumina surface* (*surface* P1). This surface consisted of a 1.3-cm-thick by 6.4-cm-diameter stainless-steel substrate on which was bonded a ceramic alumina coating 0.16 cm thick (by Dresser Industries, Westboro, MA, U.S.A.). The ceramic coating was applied to the stainless substrate by spraying a series of layers. The surface so constructed consisted of a series of layered tiers each of which had randomly dispersed holes. These layers are evident as wafered regions in Fig. 2b (isolated particles are also illustrated). As shown in Fig. 2b this surface does not resemble a porous medium consisting of an array of packed spheres. Thus while the specified porosity is known (10–12%), its permeability is uncertain as discussed in Section 3.

(c) 25% *porous/alumina surface* (*surface* P2). This surface was made from a machinable ceramic material produced by Aremco Products, Inc. (Ossining, NY, U.S.A.). A disk 6.4 cm in diameter and 0.32 cm thick was machined with a 2° conical indentation to prevent droplets from sliding off. The surface was attached directly to the copper surface, without a support substrate, by two 6-32 screws. A fine gage thermocouple (0.03 mm diameter bead) was bonded to the surface 5 mm from the center.

The material structure consisted of closely packed alumina particles 5–10 μm nominal dimension as shown in Fig. 2c. As with surface P1, permeability was uncertain.

(d) 40% *porous/alumina surface* (*surface* P3). This surface was manufactured by Alcoa Aluminum (Alcoa Center, PA, U.S.A.) and is representative of a class of alumina materials, both in porosity and composition, known to be catalytic with methanol vapors at high temperatures (> 700 K). The porosity was specified to be in the range of 40–50%. The material was supplied as a disk 6.5 cm in diameter and 5 mm thick. Due to the comparatively high thermal contact resistance between the copper billet and test surface, together with the relatively large thickness of the test surface and its low thermal conductivity, the maximum temperature to which this surface could be heated was about 620 K if limitations on heater and controller temperatures were not to be exceeded.

Figure 2c shows a 35 mm photograph and electron micrograph of this surface. The surface appears granular and to consist of bonded particles on the order of 2–5 μm size.

2.3. *Experimental observations*

Figures 3 and 4 and Table 1 summarize our evaporation time measurements. Data for the P2 surface are not shown in Fig. 3 for clarity. Figure 4 shows film boiling measurements for this surface. The P2 data overlapped the P3 measurements in the wetting region, and were very close to the P1 film boiling measurements (lower) on the scale of Fig. 3. The variation of evaporation time with surface temperature for the stainless-steel, P1 and P2 surfaces followed qualitative expectations and consisted of three characteristic regions: (1) a range of surface temperatures over which droplets made direct contact with the surface; (2) a region of nucleate/transition boiling during which intermittent droplet/surface contact was made; and (3) a film evaporation region in which the droplets were levitated above the surface (except for surface P3). For this surface, only the first two evaporation modes were observed as discussed below.

The Leidenfrost temperature was measured for the surfaces studied. These data are summarized in Table 1. The importance of this temperature resides in demarcating the temperature range where spray cooling of a hot surface can be usefully applied (i.e. note the two orders of magnitude difference in evaporation time between film boiling and surface wetting in Fig. 3), and in delineating the temperature boundary between film boiling and wetting. Difficulties with measuring T_{Leid} center around the irregular behavior of the droplets near the peak evaporation time. While some droplets near the Leidenfrost point were levitated, collapse of the vapor film occurred for others with liquid seeping into the porous surface. This often resulted in part of the droplet mass being ejected from the surface (rather like a vapor explosion). T_{Leid} is also influenced by heat absorbed by the drop which causes the surface temperature to decrease. The actual Leidenfrost temperature will be lower than the apparent measured value [9]. For high thermal conductivity surfaces, the difference is small. In the present work transient surface temperatures were not measured, and T_{Leid} was taken as the initial surface temperature measured just prior to droplet impact.

Table 1. Leidenfrost temperatures of methanol on surfaces tested

ϕ (Porosity)	$T_{Leid}(\pm 5\,K)$
0.0 (stainless-steel)	443
0.1 (P1)	570
0.25 (P2)	645
0.40 (P3)	—

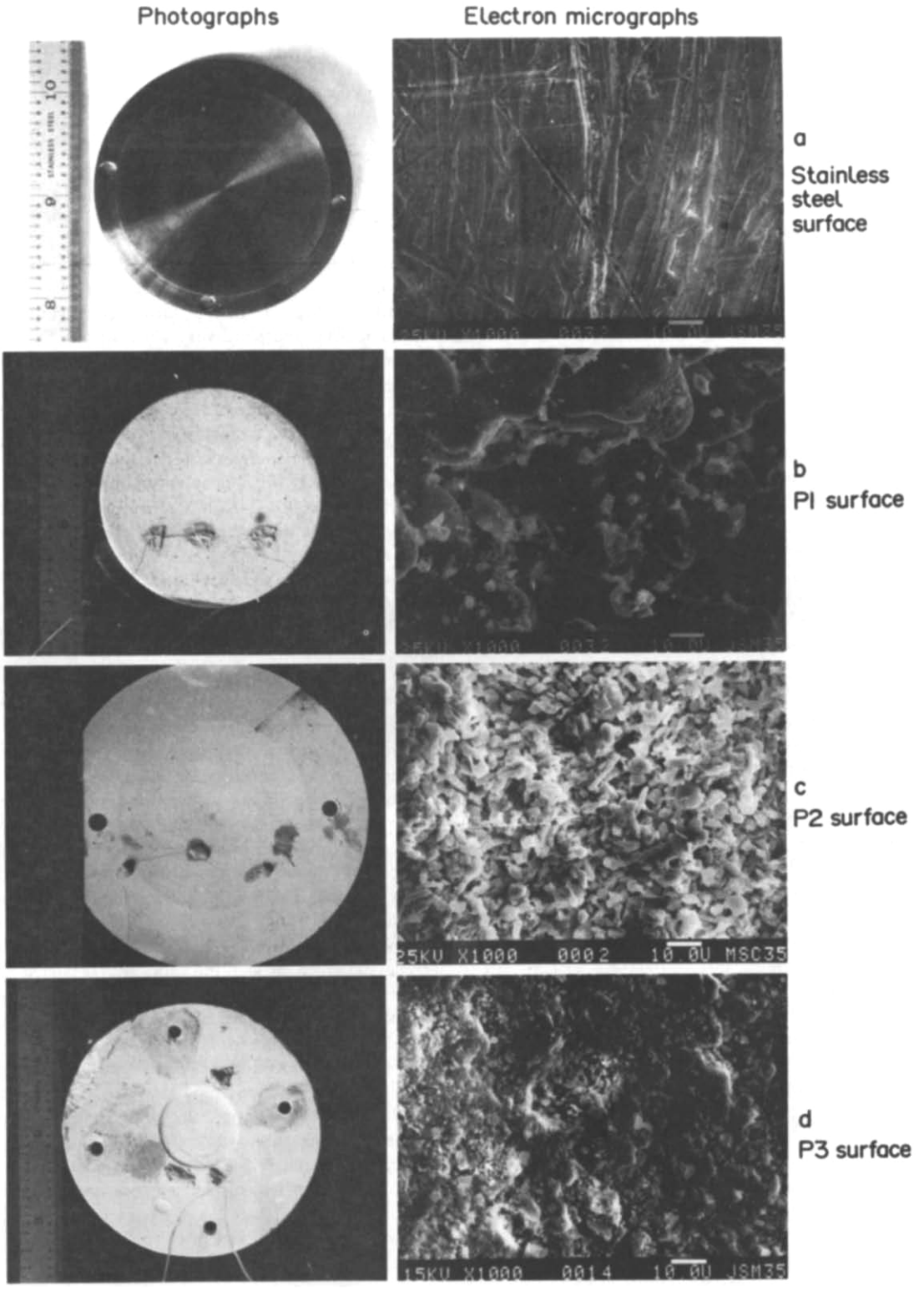

FIG. 2. 35-mm photographs and electron micrographs of test surfaces used in this study. (a) Stainless-steel; (b) 10% porous/alumina surface; (c) 25% porous/alumina surface; (d) 40% porous surface. Scale in electron micrographs (bar) indicates 10 μm.

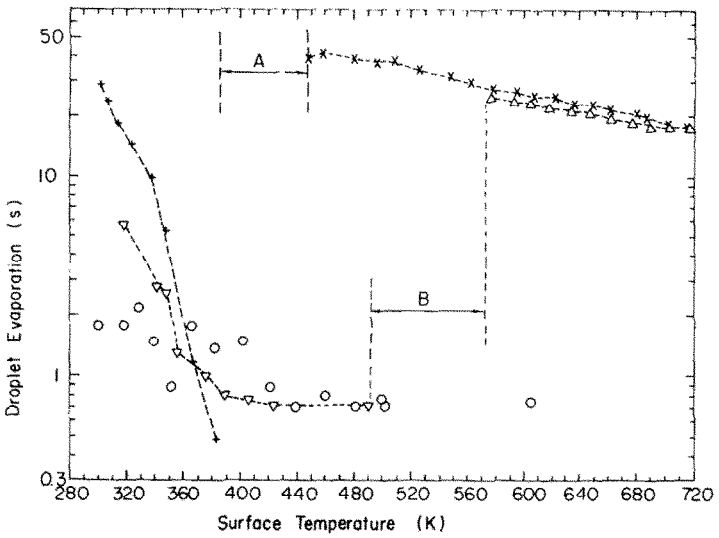

FIG. 3. Variation of evaporation time with surface temperature for methanol droplets of 11.8 μl initial volume. Stainless-steel: + wetting region; × film boiling. 10% alumina surface: ▽ wetting region; △ film boiling. 40% porous surface: ○, wetting region. Lines are drawn connecting data to illustrate the variation. A and B indicate transition boiling regime for the stainless-steel and P1 surfaces, respectively.

The Leidenfrost (i.e. initial surface) temperature for methanol on stainless-steel ($\phi = 0$) was nearly the same as previously reported for ethanol—448 K [2]—which is not unexpected. T_{Leid} has been correlated with the spinodal curve of a liquid as [9]

$$T_{\text{Leid}} = T_t \cdot f \tag{1}$$

where f is a function to account for surface thermophysical properties and $T_t = 27/32\, T_c$. Since T_c differs by only 4 K for ethanol and methanol, their Leidenfrost temperatures on stainless-steel should be nearly the same, which they were found to be.

The Leidenfrost temperature of the P3 surface was too high to be measured in our apparatus. The highest recorded surface temperature for this material was 620 K. The copper billet temperature was above 700 K. The difference between the copper and P3 surface temperature was due to the high contact resistance between the two surfaces. Severe oxidation and flaking of copper from the billet was also observed at this temperature. All droplets studied on the P3 surface therefore wet the surface. This accounts for the nearly two orders of magnitude reduction in evaporation time at the same temperatures at which stable film boiling existed on the other surfaces as shown in Fig. 3.

T_{Leid} was found to increase with porosity as shown in Table 1, and the temperature range over which

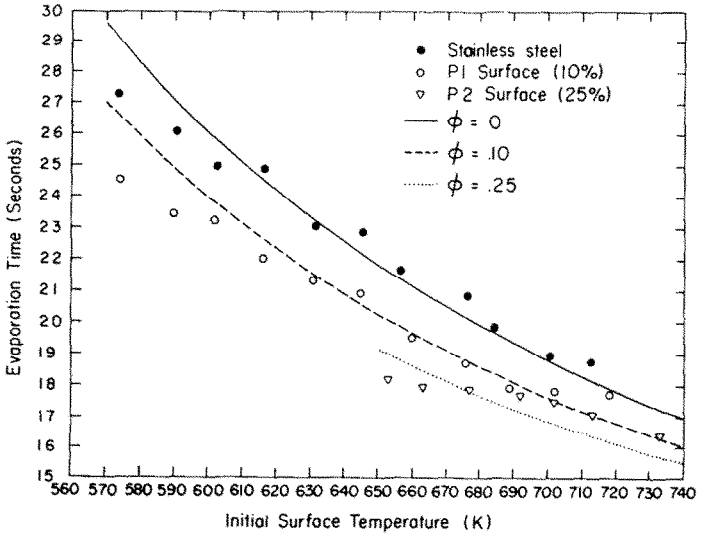

FIG. 4. Variation of evaporation time with surface temperature for methanol on stainless-steel (●), surface P1 (○) and surface P2 (▽) in the film boiling region.

droplets wet the surfaces tested increased as porosity increased. At higher porosities, more vapor can be absorbed in the solid thus requiring a higher evaporation rate to maintain levitation. This in turn will generally require a higher heat transfer rate to the droplet, and thus a higher surface temperature for levitation. The higher values of T_{Leid} measured for the P1 and P2 surfaces compared to stainless-steel suggest that porosity be included in the functional dependence for f, though the precise form of this dependence requires more data.

At temperatures below T_{Leid}, a region characterized by unstable or transition boiling was observed. Liquid was simultaneously absorbed and evaporated, thus making it more difficult to unambiguously determine the evaporation time (for this reason no data are reported in regions A and B in Fig. 3). For example, Fig. 5 illustrates a sequence of 35 mm photographs (at 5 frames s^{-1}) of methanol droplets evaporating on surface P1 at the indicated surface temperatures. (Results shown in Figs. 4a and b were similar to those observed for surfaces P2 and P3.) In the wetting regime but below the normal boiling point of methanol (338 K), liquid was absorbed into the P1 surface and spread out while simultaneously evaporating (note spreading of the ring around the puddle in the first frame of Fig. 5a). For purposes of relative consistency in these cases (or surfaces P2 and P3 as well) the apparent evaporation time of the droplet was recorded. We defined this as the time from initial surface contact at which all liquid matter appeared to disappear from the visible surface. The time progressively approached the actual evaporation time as surface temperature increased. For example, at 435 K (Fig. 5b—above the boiling point) evaporation was fast enough to prevent significant spreading of absorbed liquid so that no ring was visible. The time for disappearance of the deposited liquid nearly coincided (to ± 0.1 s) with disappearance of the observed dryout front (cf. Figs. 5a and b). These two times progressively diverged as surface temperature was decreased below about 375 K. We could not then be confident that evaporation of liquid absorbed within the ceramic (Fig. 5a) coincided with disappearance of the liquid from the surface at low temperatures; measurements in this temperature range are therefore the most uncertain.

In the transition region (Figs. 5c and d) droplets either randomly wetted the surface (Fig. 5c) or were levitated (Fig. 5d). When they wet, vigorous nucleate boiling occurred and liquid had the appearance of a foam caused by bubbles passing through the drop (the white central region in Fig. 5c). The effect of wetting near T_{Leid} was to cause the droplets to rapidly seep (i.e. 'fizz') into the ceramic. This occurred in a random manner, as sometimes droplets would also be levitated during evaporation (cf. Fig. 5d) in the transition region. Occasionally, droplets remained levitated throughout evaporation in the transition region (Fig. 5d). Above T_{Leid}, droplets were always levitated. A mechanism for this subsequent wetting after initial levitation is offered in the next section which involves a combination of increased surface porosity and heat transfer into the surface.

In the stable film boiling region, droplets evaporated on the ceramic surfaces in a manner similar to that observed on stainless-steel. However, the evaporation times were lower as shown in Fig. 4. A model to explain this reduced evaporation time is discussed in the next section.

3. ANALYSIS AND CORRELATION OF FILM BOILING DATA

The analysis here focuses on the film boiling regime. Closed form solutions to this problem (liquid droplets) have only been obtained for two limiting cases: (1) the droplet is a rigid sphere and Stokes flow exists in the gas phase [11]; and (2) potential flow in the gas phase [12]. More approximate treatments have been successful in providing a basis for empirical correlations [1–4]. These studies assumed that flow in the vapor film which separates the droplet from the hot surface resembled fully developed laminar flow between parallel plates. Flow in the film is fed by evaporation from the underside of the droplet, and the corresponding pressure gradient provides the force which levitates the droplet above the surface. This approach is here modified to account for the presence of the porous surface and heat transfer into the surface.

Figure 6 illustrates the model. A liquid droplet is separated from a porous surface by a vapor film. The film is supported by evaporation from the base of the droplet, and some of this vapor is absorbed in the porous material. The problem is to predict the velocity, pressure distribution beneath the droplet, film thickness, heat transfer rate into the surface and the droplet evaporation rate.

Several assumptions employed in previous studies of droplets evaporating on impermeable surfaces are the following (e.g. [1–4]): (1) the vapor film of thickness δ is very thin so that conduction dominates at any time and radiation is negligible; (2) the droplet is in the shape of a truncated oblate spheroid; (3) mass diffusion over the upper surface of the droplet and transient droplet heating are neglected; (4) the film thickness is assumed uniform; and (5) the solid surface temperature is independent of time. The neglect of radiation is justified for the temperatures of interest here (<700 K): $\sigma\gamma(T_{s0}^4 - T_b^4)/[k_g(T_{s0} - T_b)/\delta] \ll 1$, and considering the view factor associated with the upper surface, a similar small ratio of radiation (to the sides) to conduction across the film could be demonstrated. The neglect of mass diffusion may not be justified, but its effect has been shown to be essentially a multiplying factor to the evaporation time [3] and could, if included in the present treatment, be absorbed in our correlating variable. The initial sessile configuration of a droplet is similar to a truncated

oblate spheroid (see Fig. 6a), though assuming other geometric shapes would not alter the qualitative results. Truncation factors were fixed as $\Phi \simeq 0.48$ and $\alpha = 1.42$ (based on photographs). An analysis which neglects transient droplet heating is reasonable inasmuch as the initial subcooling was only 5 K. Finally, heat transfer from the surface to the droplet will cause the surface temperature to decrease from its initial value in the region around the evaporating droplet. This effect could be significant for refractory type materials with low thermal conductivities. For Al_2O_3 ceramics of the type used here, the dense (i.e. zero porosity) thermal conductivity can actually be of the same order as that of stainless-steel, though the effect

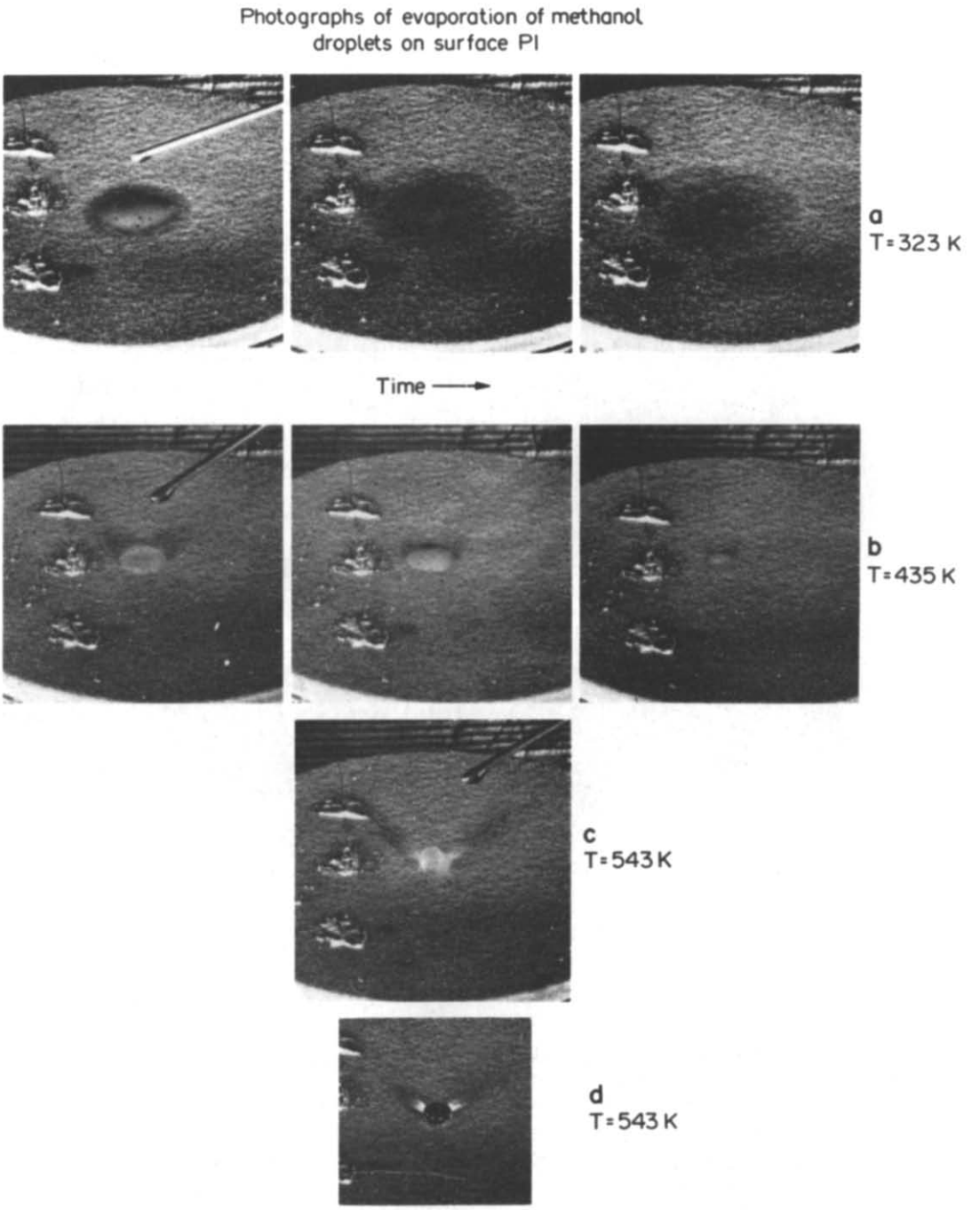

FIG. 5. Series of 35 mm photographs at 5 frames s^{-1} of an overhead view with front lighting of evaporation of 11.8 μl of methanol on surface P1. 18 gage needle is visible in first frames in figs (a)–(c). (a) Wetting and spreading of liquid ($T_{so} < T_b$). (b) Wetting region without significant spreading while evaporating (liquid is the central white region) at $T_{so} > T_b$. (c) Transition region evaporation with wetting and bubbling on contact (white central region). (d) Film evaporation in transition region.

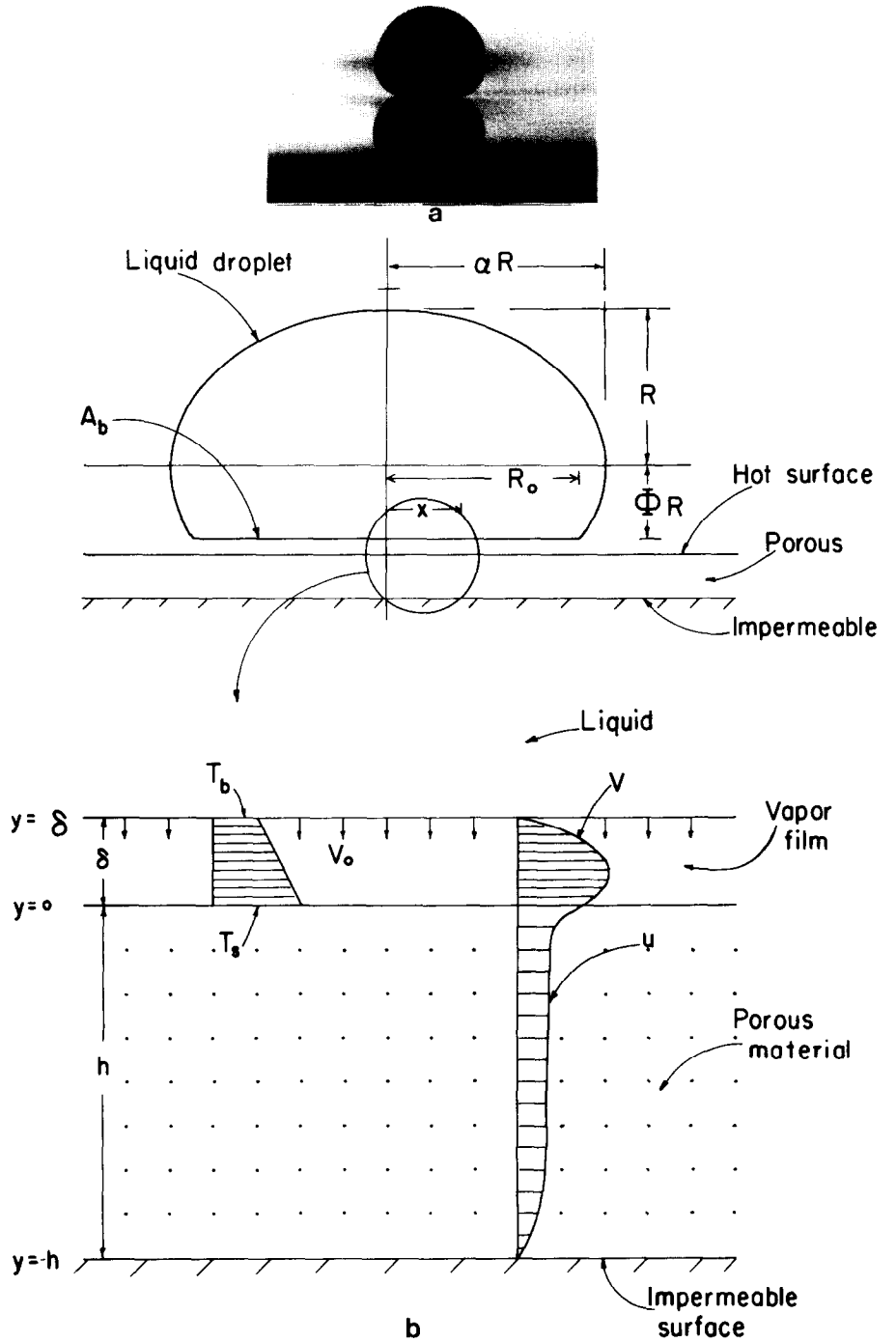

FIG. 6. Model of a levitated droplet. (a) Backlighted 35 mm photograph of a methanol droplet above stainless-steel taken along the plane of the surface (the same as on surfaces P1 and P2). Note the vapor film. (b) Model of a levitated droplet (not to scale).

of porosity on thermal properties could likely result in deviations which would cause significant surface temperature decreases during evaporation.

The momentum equation for flow in a porous medium relevant to the present problem is [13]

$$\nabla^2\bar{v} = \frac{\phi}{\mu}\nabla P + \frac{\bar{v}}{k} \qquad (2)$$

where $k = \bar{k}/\phi$, $\bar{k}$ is the permeability (cm^2), and ϕ is the porosity. For the vapor film and the porous substrate, the one-dimensional simplification of equation (2) is

$$\frac{d^2v}{dy^2} = \frac{1}{\mu}\frac{dP}{dx} \qquad (3)$$

$$\frac{d^2u}{dy^2} = \frac{\phi}{\mu}\frac{dP}{dx} + \frac{u}{k}. \tag{4}$$

The boundary conditions are

$$v(\delta) = 0 \tag{5a}$$

$$u(0) = v(0) \tag{5b}$$

$$\left.\frac{du}{dy}\right|_{y=0} = \varepsilon\left.\frac{dv}{dy}\right|_{y=0} \tag{5c}$$

$$u(-h) = 0. \tag{5d}$$

Boundary condition (5a) is more realistic than allowing for slip at the interface in view of the large difference between the liquid and vapor viscosity [4]. Boundary condition (5c) is like a matching condition for fluid stress at the boundary of the porous surface and vapor film [14] though alternative coupling conditions have been used [15, 16].

If the momentum transport at the interface between the vapor film underneath the droplet and porous surface is continuous, then $\varepsilon = 1$. However, if the vapor flow in the film is considered to transfer momentum not only to the fluid within the rigid porous medium, but also to the solid matrix itself then $\varepsilon < 1$. A value is indeterminate from available information except insofar as ε might be inferred from measurements of evaporation times. Since the results were found to be insensitive to ε in the range $0 < \varepsilon < 1$, $\varepsilon \simeq 1$ was assumed in the present work.

The problem as formulated is similar to flow in a semi-infinite ($h \to -\infty$) porous matrix over which a viscous fluid flows [17]. Here, the thickness of the porous medium is finite and the fluid is bounded above by a solid wall (i.e. the droplet base).

The solutions to equations (3)–(5) are

$$v = \frac{1}{\mu}\frac{dP}{dx}\cdot\left(\frac{y^2}{2} + a_1 y + a_2\right) \tag{6}$$

and

$$u = \frac{1}{\mu}\frac{dP}{dx}(b_1 e^{y/k^{1/2}} + b_2 e^{-y/k^{1/2}} - \phi k) \tag{7}$$

where

$$a_1 = [(2k\phi - \delta^2)(1 - e^{-2\zeta}) - 4k\phi e^{-\zeta}]/\Delta \tag{8a}$$

$$a_2 = [-k^{1/2}\varepsilon\delta(1 - e^{-2\zeta}) + 4\delta k e^{-\zeta} - 2\phi\delta k(1 + e^{-2\zeta})]/\Delta \tag{8b}$$

$$b_1 = \{\varepsilon k^{1/2}[2\phi k(1 - e^{-\zeta}) - \delta^2] + 2\phi\delta k e^{-\zeta}\}/\Delta \tag{8c}$$

and

$$b_2 = \{\varepsilon k^{1/2}[2\phi k e^{-\zeta} + e^{-2\zeta}(\delta^2 - 2\phi k)] + 2\phi\delta k e^{-\zeta}\}/\Delta \tag{8d}$$

$$\Delta = 2[\varepsilon k^{1/2}(1 - e^{-2\zeta}) + \delta(1 + e^{-2\zeta})] \tag{8e}$$

where

$$\zeta = h/k^{1/2}.$$

Though $\zeta \gg 1$, this limit cannot be taken before calculating the mass flow rates through the vapor film and ceramic layer. These flow rates are

$$\dot{m}_v = 2\pi x\rho_v \cdot \frac{1}{\mu}\frac{dP}{dx}\left(\frac{\delta^3}{6} + a_1\frac{\delta^2}{2} + a_2\delta\right) \tag{9}$$

and

$$\dot{m}_u = 2\pi x\rho_v \cdot \frac{1}{\mu}\frac{dP}{dx}[b_1 k^{1/2}(1 - e^{-\zeta}) - b_2 k^{1/2}(1 - e^{\zeta}) - \phi hk]. \tag{10}$$

The flow in the film and porous layer is assumed to be driven by evaporation at the base of the droplet. Hence

$$\rho_v v_0 \cdot \pi x^2 = \dot{m}_v + \dot{m}_u \tag{11}$$

where the vertical vapor velocity based on a simple conduction model is

$$v_0 \simeq \frac{k_g \Delta T}{\rho_v h_{fg}\delta} \tag{12}$$

and $\Delta T \equiv T_s - T_b$.

The pressure distribution in the vapor film produces an upward force at the base of the droplet which is counterbalanced by the weight of the droplet. For a horizontal surface,

$$\int_A (P - P_0)\cdot 2\pi x\,dx = g\rho_l - \rho_g V \tag{13}$$

Combining equations (8)–(12), integrating to determine $P - P_0$, substituting the result in equation (13), and taking the limit $\zeta \gg 1$ [i.e. $h \sim \theta(1\,\text{mm})$ and $k \sim \theta(10^{-9}\,\text{cm}^2)$], yields a relation between δ and V as

$$\frac{1}{6}\delta^5 - \delta^4 k^{1/2}\left(\frac{1}{3} - \varepsilon\right) + \delta^3 k(\phi + \varepsilon) + \delta^2\cdot 2k(h\phi - k^{1/2}) - \delta 2[\Delta T B V^{1/3} + \phi k^{3/2}\varepsilon(2k^{1/2} - h)] + 2B\varepsilon k^{1/2} V^{1/3}\Delta T = 0 \tag{14}$$

where

$$B = \frac{1}{8}\left(\frac{3f_2^{3/2}}{4\pi f_1}\right)^{4/3}\cdot\frac{\pi k_g \mu_g}{h_{fg}\rho_l\rho_g g} \tag{15}$$

and f_1 and f_2 are volume and surface area truncation factors for an oblate spheroid. Equation (14) reduces to an expression for δ previously derived [3] in the limit of an impermeable surface:

$$\delta = (12B\Delta T)^{1/4}\cdot V^{1/12}. \tag{16}$$

Several qualitative characteristics of levitation can be illustrated from equation (14). If the surface temperature is too low, or its porosity too high, a droplet will not be levitated, that is, it will initially impact the surface. In this case, either no solution or a negative root of equation (14) would result. Figure 7 illustrates

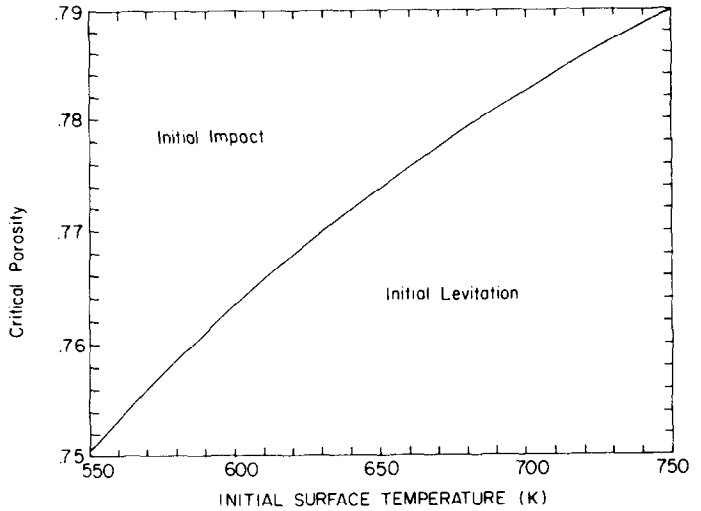

FIG. 7. Variation of porosity above which a droplet is not initially levitated with initial surface temperature. $l = 10\,\mu$m and $\alpha = \alpha_{ss}$ assumed for illustration.

the variation of a critical porosity above which a droplet would not be initially levitated [$\delta_i \equiv \delta(V = V_0) \to 0$] with initial surface temperatures [$T_s(t = 0)$] which span the range of our film evaporation data. In this figure the Kozeny–Carman relation was used to relate k to ϕ [18]:

$$k = \frac{l^2}{C_0}\frac{\phi^2}{(1-\phi)^2} \tag{17}$$

where l is a length scale characteristic of the solid matrix (particle volume/particle surface area). The use of equation (17) is only approximate as none of the porous surfaces used (Fig. 2) resembled an array of spheres and no data on their permeabilities were available. It is known [19] that equation (17) yields high values of permeability when applied to porous materials of nonuniform particle size or in which there is significant cementation. Using equation (17) is, therefore, only an attempt to obtain a rough estimate of k. Though estimated values are probably not accurate to more than an order of magnitude, the qualitative form of the solution presented would not be altered with other choices. The existence of a critical surface porosity for levitation at a given temperature partially explains the observation that film boiling on the P3 surface did not occur for the range of surface temperatures tested. The porosity may have been too high to support both the pressure gradient which lifts the droplet above the surface and the flow of absorbed vapor through the surface.

l was selected to be a characteristic dimension as $l \simeq 10\,\mu$m (for illustration), and C_0 was chosen to be characteristic of a matrix of packed spheres as 180 when l is sphere diameter [18].

Figures 8 and 9 illustrate variations of initial levitation height with surface temperature (when $\phi = 0.1$ for illustration) and porosity (at two initial surface temperatures), respectively. Figure 8 shows that a droplet initially resides progressively closer to

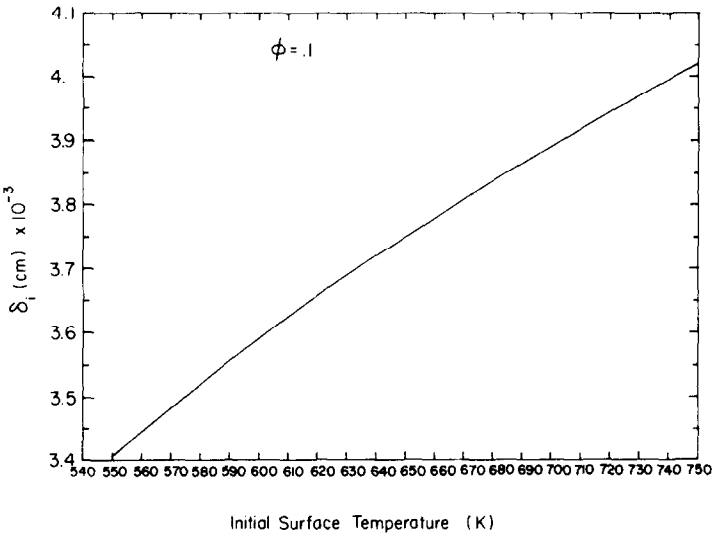

FIG. 8. Effect of initial surface temperature on initial levitation height for a 10% porous surface. $l = 10\,\mu$m and $\alpha = \alpha_{ss}$.

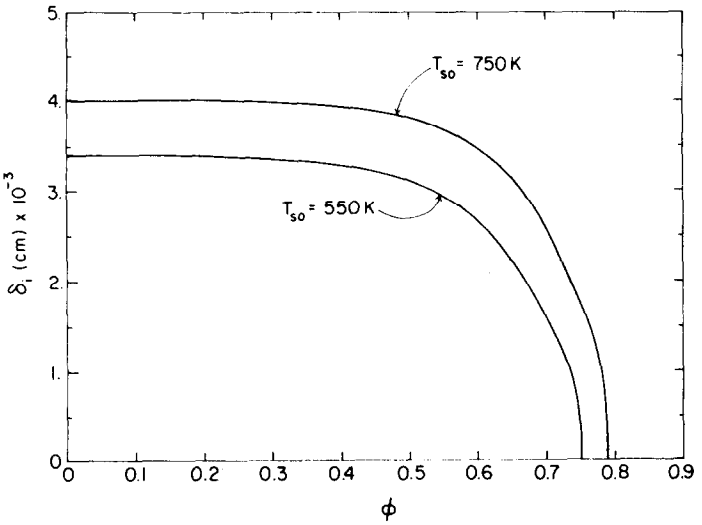

FIG. 9. Variation of initial levitation height with porosity at surface temperatures of 550 and 750 K. When $\delta_i = 0$, droplet is not levitated.

the surface as initial surface temperature decreases. This is because with a lower surface temperature and $q \sim (T_s - T_b)/\delta$ the levitation height must be reduced if T_s is lowered to maintain the evaporation which creates the vapor flow and pressure gradient that balances the droplet weight. The droplet also resides closer to the surface as porosity increases for constant initial surface temperature (Fig. 9) because of increased vapor percolation into the surface. The droplet must evaporate faster, hence reside closer to the surface (where heat transfer to it increases), to overcome an effective vapor 'loss' into the surface. Eventually, at a high value of ϕ (the critical porosity), $\delta_i = 0$ and the droplet cannot be levitated at the respective surface temperature.

To determine the total droplet evaporation time, a heat/mass balance at the base of the droplet yields

$$\frac{dV}{dt} = -\xi \frac{k_g V^{2/3}}{h_{fg}\rho_l} \frac{T_s - T_b}{\delta} \tag{18}$$

where

$$\xi = \left(\frac{3\pi^{1/2}}{4}\frac{f_2^{3/2}}{f_1}\right)^{2/3} \tag{19}$$

and is a geometric factor. The surface temperature will drop during evaporation because of the finite heat transfer rate through the surface and the heat absorbed by the droplet. This problem has been addressed by Baumeister and Simon [9] in which it was shown that if $\eta \equiv HR_0/k_s \geq 2$ heat transfer from the surface can be modelled as a semi-infinite solid characterized by an 'ambient' at T_b and a heat transfer coefficient H. In the present problem, the ambient is effectively located a distance δ from the surface so that we take

$$H \simeq \frac{k_g}{\delta}. \tag{20}$$

For $k_g \sim 10^{-4}$ cal cm^{-1} s^{-1} °C^{-1}, $k_s \sim 10^{-2}$ cal cm^{-1} s^{-1} °C^{-1}, $\delta \sim 10^{-3}$cm [12], and $R_0 \sim 0.5$ cm, then $\eta \sim 20$. To simplify further the thermal analysis for the solid, we will employ a kind of quasi-steady assumption wherein δ is a constant in the energy equation for the solid while its time dependent behavior is determined by an energy balance on the drop [equation (18)]. This assumption will still preserve the general characteristics of a more precise solution. The surface temperature can then be written as [20]

$$T_s \simeq T_b + (T_{so} - T_b)\exp\left(\frac{k_g^2}{\delta^2}\frac{t}{\alpha}\right)\text{erfc}\left[\frac{k_g}{\delta}\left(\frac{t}{\alpha}\right)^{1/2}\right] \tag{21}$$

where $\alpha \equiv k_s\rho_s C_{ps}$.

Equations (18)–(21) were solved numerically using a fourth-order Runge–Kutta method with a time step of 0.2 s. Physical properties for methanol vapor and stainless-steel used in the calculations are listed in Table 2. Unfortunately, no reliable data could be found for the variation of thermal properties with porosity for the ceramics used in this study. The basis of our empirical correlation, therefore, was to consider ξ and α adjustable constants whose values were selected to give optimum agreement with the evaporation time measurement. Assuming ξ is independent of porosity, a value was determined by the film evaporation data for methanol on stainless-steel ($\phi = 0$). $\xi \simeq 1.07$ was found to best correlate these data as shown in Fig. 4 (solid line). α is a function of surface porosity. An empirical correlation of the

Table 2. Properties

Methanol
$\rho_l = 0.773$ g cm^{-3} (337 K)
$h_{fg} = 264.56$ cal gm^{-1} (337 K)
$k_g = 7.96 \times 10^{-5}$ cal cm^{-1} s^{-1} °C^{-1} (525 K)
Stainless-steel at 525 K
$\rho_s = 7.9$ g cm^{-3}
$C_{ps} = 0.128$ cal gm^{-1} °C^{-1}
$k_s = 0.0435$ cal cm^{-1} s^{-1} °C^{-1}

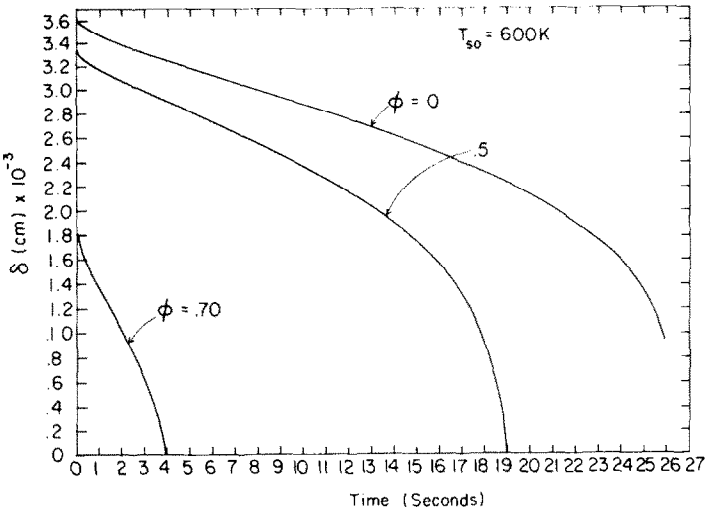

FIG. 10. Temporal variation of levitation height for the indicated porosities and $T_{s0} = 600$ K. When $\delta = 0$, droplet impacts the surface.

Leidenfrost evaporation data for the P1 and P2 surfaces yielded $\alpha \simeq \alpha_{ss}(1 + 5\phi)$ where α_{ss} is the thermal diffusivity of stainless-steel. $l \simeq 50\,\mu$m for surface P1 and $l = 10\,\mu$m for surface P2 were assumed. Figure 4 shows predictions based on this correlation for the P1 (dashed line) and P2 (dotted line) surfaces. The solution was carried out until $V = 0$, which defines the total evaporation time.

To illustrate the temporal variations of δ, equivalent droplet diameter (based on volume), and T_s, a hypothetical surface at an initial temperature of 600 K and with $\alpha(=\alpha_{ss})$ independent of porosity was selected. To assume otherwise for α would not alter the form of these calculations, nor necessarily improve their quantitative accuracy because of the uncertainty in thermal properties of the ceramics used. The porosity effect was then carried in δ [equation (14)] and k. The variation of δ with time shown in Fig. 10 indicates that as porosity increases δ can vanish before complete evaporation ($V = 0$) even though the droplet may initially be levitated. The droplet then impacts the surface. This result is consistent with several experimental observations which showed that droplets sometimes wetted and seeped into the ceramic surfaces after initial levitation. For stainless-steel ($\phi = 0$) a droplet initially levitated would remain so throughout evaporation. It is perhaps worth mentioning that the calculated decrease of levitation height with time shown in Fig. 10 is characteristic of a model for film evaporation which assumes the base of the droplet is flat, the vapor flow is laminar in the film, and heat transfer occurs only to this base (e.g. [3, 5]).

Figure 11 shows the variation of equivalent diameter with time. The termination of the two curves corresponding to $\phi = 0.5$ and 0.75 coincides with the droplet impacting the surface ($\delta = 0$ in Fig. 10). For $\phi = 0$ evaporation goes to completion (diameter = 0). Figure 12 shows the variation of surface temperature

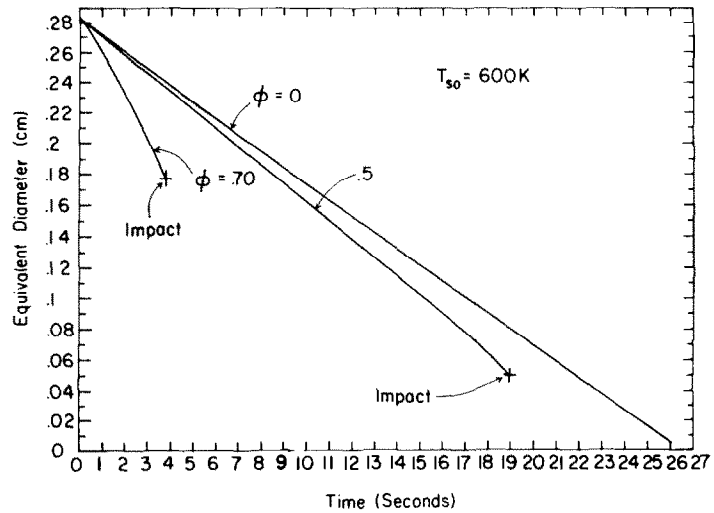

FIG. 11. Variation of droplet diameter (based on the volume V of an oblate spheroid) with time for three different porosities and $T_{s0} = 600$ K. Termination of calculations for $\phi = 0.5$ and 0.7 coincide with $\delta = 0$ in Fig. 10.

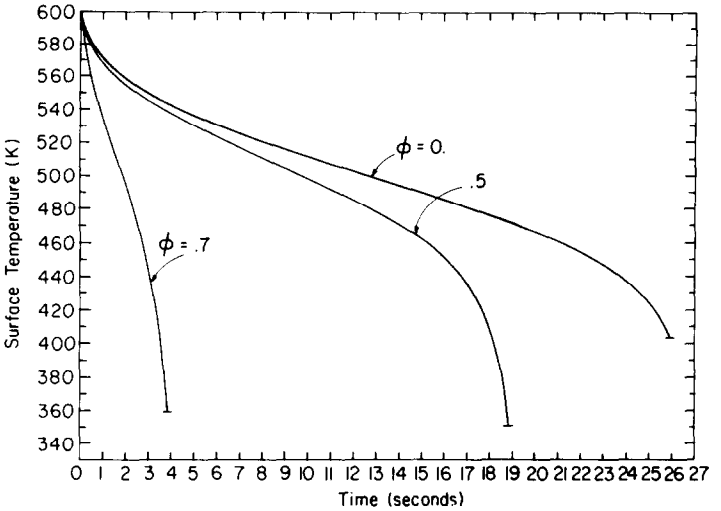

FIG. 12. Variation of surface temperature with time at three different porosities. $l \simeq 10\,\mu m$ and $\alpha = \alpha_{ss}$.

with time for this hypothetical material ($\alpha = \alpha_{ss}$). Again, the calculations were terminated when the droplet completely evaporated ($\phi = 0$) or impacted the surface ($\phi = 0.5, 0.75$).

The present results are perhaps useful for understanding, and to a certain extent predicting, the effect of porosity on the evaporation time of a liquid droplet in film boiling on a horizontal, permeable surface. Though the dominant mechanisms which control this evaporation are accounted for—vapor percolation, flow, and heat transfer in the porous surface—the present model must be considered as representing only part of the physics of film evaporation at a porous surface, and only partly as modelling the entire process. A more exact treatment, starting from the governing equations in their full form, would eliminate the existence of empirical constants. More data also need to be obtained on the dependence of thermal properties on porosity, and the permeability of ceramic materials.

4. CONCLUSIONS

Evaporation of methanol droplets on ceramic/porous surfaces was studied. Results showed that in the film boiling region methanol evaporated faster above a porous/alumina surface than above an impermeable surface at the same surface temperature.

For an alumina silicate surface of 40% porosity, deposited droplets did not levitate but instead directly contacted the surface at all surface temperatures studied. The corresponding evaporation times were nearly two orders of magnitude lower than those measured for film boiling on the stainless-steel, 10%, and 25% porous/alumina surfaces at the same surface temperatures.

A simple model based on vapor absorption, flow, and heat transfer in a porous surface and a vapor film showed that a droplet in film evaporation resides closer to a porous surface than an impermeable surface at the same surface temperature. This results in a decrease in the evaporation time as experimentally observed. The model also provided a mechanism for droplet impact with the surface during evaporation.

Acknowledgements—The authors thank Dr Nancy Fitzgerald of Alcoa Aluminum Company for her interest in our work and for supplying us with the 40% porous ceramic/alumina surface. Conversations with Professor Kenneth E. Torrance of Cornell, and the comments of a reviewer, have been helpful. This work was supported by a grant from the Exxon Research and Engineering Company with Mr A. R. Tenner as project monitor. The videotape equipment was purchased under Equipment Grant No. CBT-8305263 from the Thermodynamics and Transport Phenomena Program of the National Science Foundation. This support has been greatly appreciated.

REFERENCES

1. B. S. Gottfried, C. J. Lee and K. J. Bell, The Leidenfrost phenomenon: film boiling of liquid droplets on a flat plate, *Int. J. Heat Mass Transfer* **9**, 1167–1187 (1966).
2. E. S. Godleski and K. J. Bell, The Leidenfrost phenomenon for binary liquid solutions, *Proc. 3rd Int. Heat Transfer Conference* Vol. 4, pp. 51–58.
3. B. S. Gottfried and K. J. Bell, Film boiling of spheroidal droplets, *Ind. Engng chem. Fundam.* **5**, 561–568 (1966).
4. K. J. Bell, The Leidenfrost phenomenon: a survey, *Chem. Engng Prog. Symp. Ser.* **63**(79), 73–82 (1967).
5. C. T. Avedisian, C. Ioffredo and M. J. O'Connor, Film boiling of discrete droplets of mixtures of coal and water on a horizontal brass surface, *Chem. Engng Sci.* **39**, 319–327 (1984).
6. S. A. Sheffield, M. R. Baer and C. J. Denison, Papers No. 42 and 43, Fall Technical Meeting, The Eastern Section of the Combustion Institute, Princeton (November 1980).
7. P. Cho and C. L. Law, Pressure/temperature ignition limits of fuel droplet vaporizing over a hot plate, *Int. J. Heat Mass Transfer* **28**, 2174–2176 (1985).
8. G. S. Emmerson, The effect of pressure and surface material on the Leidenfrost point of discrete drops of water, *Int. J. Heat Mass Transfer* **18**, 381–386 (1975).
9. K. J. Baumeister and F. F. Simon, Leidenfrost temperature—its correlation for liquid metals, cryogens, hydrocarbons and water, *J. Heat Transfer* **95**, 166–173 (1973).

10. R. F. Probstein, *Synthetic Fuels*, p. 130. McGraw-Hill, New York (1982).
11. A. K. Sen and C. K. Law, On a slowly evaporating droplet near a hot plate, *Int. J. Heat Mass Transfer* **27**, 1418–1421 (1984).
12. J. Kistemaker, The spheroidal state of a waterdrop, *Physica* **29**, 96–104 (1963).
13. K. Vafai and C. L. Tien, Boundary and inertia effects on flow and heat transfer in a porous media, *Int. J. Heat Mass Transfer* **24**, 195–203 (1981).
14. K. E. Torrance, Private communication (April 1985).
15. B. E. Eidelberg and J. F. Booker, Application of finite element methods to lubrication: squeeze films between porous surfaces, *J. Lub. Tech.* 175–186 (January 1976).
16. G. S. Beavers and D. D. Joseph, Boundary conditions at a naturally permeable wall, *J. Fluid Mech.* **30**, 197–207 (1967).
17. G. I. Taylor, A model for the boundary condition of a porous material. Part 1, *J. Fluid Mech.* **49**, 319–326 (1971).
18. J. Bear, *Dynamics of Fluids in Porous Media*, pp. 165–168. Elsevier, New York (1972).
19. C. S. Brooks and W. R. Purcell, Surface area measurements on sedimentary rocks. *Trans. Am. Inst. Min. Engrs* **195**, 289–296 (1952).
20. H. S. Carslaw and J. C. Jaeger, *Conduction of Heat in Solids*, 2nd edn, p. 71. Clarendon Press, Oxford (1959).

EBULLITION DES GOUTTELETTES DE METHANOL SUR DES SURFACES CHAUDES, POREUSE, DANS LE REGIME DE LEIDENFROST

Résumé—On présente une étude expérimentale et analytique de l'ébullition en film de gouttelettes de méthanol sur une surface en céramique poreuse. Les temps d'évaporation de gouttelette, dans les régimes de mouillage et d'ebullition en film, sont mesurés sur une surface d'acier inoxydable et sur trois surfaces de céramiques poreuses en alumine avec des porosités de 10, 25 et 40%. On trouve que les températures de Leidenfrost augmentent lorsque la porosité croît. Les points de Leidenfrost des surfaces à 10 et 25% de porosité sont respectivement supérieurs de près de 100 et 200 K à celui de la surface polie d'acier inoxydable. Le temps de'évaporation du liquide déposé sur cette surface est deux fois plus faible de celui des gouttelettes sur les trois autres surfaces portées à la même température. Les temps réduits d'évaporation doivent avoir leur origine dans la diminution de l'épaisseur du film de vapeur séparant la gouttelette de la surface céramique, à cause de l'absorption de la vapeur et de l'écoulement dans le matériau poreux. Une analyse de l'écoulement dans un canal horizontal limité par une paroi imperméable sur le dessus et une paroi perméable d'épaisseur finie au-dessous, est faite pour représenter l'ébullition en film. Les résultats fournissent une base pour relier entre eux les temps d'évaporation mesurés.

VERDAMPFUNG VON METHSANOLTROPFEN AM LEIDENFROST-PUNKT AN HEISSEN PORÖSEN KERAMIKOBERFLÄCHEN

Zusammenfassung—Es wird über eine experimentelle und analytische Untersuchung zum Filmsieden von Methanoltropfén an porösen Keramikoberflächen berichtet. Die Verdampfungszeiten der Tropfen im benetzten und im Filmsiede-Bereich wurden an Oberflächen von poliertem nichtrostendem Stahl und an drei Keramik/Aluminium-Oberflächen mit 10, 20 und 40% Porosität gemessen. Es wurde festgestellt, daß die Leidenfrost-Temperatur mit zunehmender Oberflächenporosität ansteigt. Der Leidenfrost-Punkt der 10 bzw. 20% porösen Oberflache lag nahezu 100 bzw. 200 K höher als derjenige der polierten Oberfläche von nichtrostendem Stahl. An der 40% porösen Oberfläche konnten die Methanoltropfen bei einer Oberflächentemperatur von 620 K nicht in den Schwebezustand versetzt werden. Dies war die maximale Temperatur, die in der vorhandenen Anlage für das verwendete Material aufgebracht werden konnte. Die Verdampfungszeiten von Flüssigkeitsanlagerungen an dieser Oberfläche waren daher bei gleicher Temperatur fast zwei Größenordnungen neidriger als für schwebende Tropfen an den drei anderen Oberflächen. Im Leidenfrost-Gebiet verdampften die Tropfen an den porösen Oberflächen schneller als an der Oberfläche von nichtrostendem Stahl. Die Verdampfungszeit verkürzte sich bei gleicher Oberflächentemperatur mit zunehmender Oberflächenporosität. Es wird angenommen, daß die verkürzten Verdampfungszeiten von dem—aufgrund von Dampfabsorption und Dampfströmung in das Keramikmaterial—dünner werdenden Dampffilm, der die Tropfen von der Keramikoberfläche trennt, herrührt. Eine Untersuchung der Strömung in einem horizontalen Kanal, der oben von einer underchlässigen Wand und unten von einer durchlässigen Wand endlicher Dicke begranzt wird, wurde benutzt, um den Filmsiedeprozeß zu modellieren. Die Ergebnisse brachten eine Grundlage zur Korrelation der Verdampfungszeitmessungen.

КИПЕНИЕ КАПЕЛЬ МЕТАНОЛА В РЕЖИМЕ ЛЕЙДЕНФРОСТА НА НАГРЕТЫХ ПОРИСТЫХ/КЕРАМИЧЕСКИХ ПОВЕРХНОСТЯХ

Аннотация—Экспериментально и теоретически исследовалось пленочное кипение капель метанола на пористой (керамической) поверхности. Измерялось время испарения капель в режимах смачивания и пленочного кипения на полированной поверхности из нержавеющей стали и трех керамических (корундовых) поверхностях с пористостью 10, 25 и 40%. Найдено, что температура Лейденфроста увеличивалась с ростом пористости поверхности. Точки Лейденфроста для поверхностей с пористостью 10 и 25% были, соответственно, почти на 100 и 200 К выше, чем для полированной поверхности из нержавеющей стали; капли метанола не витали над поверхностью с пористостью 40% при температуре поверхности в 620 К, которая была максимально допустимой в используемой экспериментальной установке. Таким образом, время испарения нанесенной на эту поверхность жидкости было почти на два порядка меньше, чем для капель, витающих над

тремя другими поверхностями, которые исследовались при той же температуре. В режиме Лейденфроста капли испарялись быстрее на пористых поверхностях, чем на поверхности из нержавеющей стали, и время испарения уменьшалось с увеличением пористости при той же температуре поверхности. Высказано предположение, что уменьшение времени испарения происходит из-за уменьшения толщины пленки пара, отделяющей каплю от керамической поверхности вследствие абсорбции пара, и течения внутрь керамического материала. Для моделирования процесса пленочного кипения анализировалось течение в горизонтальном канале, ограниченном непроницаемой стенкой сверху и проницаемой стенкой конечной толщины снизу. Результаты позволили обобщить полученные экспериментальные данные по времени испарения.